Published in final edited form as:

Neuroimage. 2025 October 15; 320: 121458. doi:10.1016/j.neuroimage.2025.121458.

Spatiotemporal dynamics of multispectral oscillatory activity underlying the processing of negative and positive emotional images

Nathan M. Petro[a,*], **Mikki Schantell**[a], **Mia C. Lulli**[a], **Kellen M. McDonald**[a,b], **Chloe C. Casagrande**[a], **Christine M. Embury**[a], **Hannah J. Okelberry**[a], **Jason A. John**[a], **Ryan Glesinger**[a], **Lucy K. Horne**[a], **Giorgia Picci**[a,b], **Tony W. Wilson**[a,b]

[a]Institute for Human Neuroscience, Boys Town National Research Hospital, Boys Town, NE, USA

[b]Department of Pharmacology & Neuroscience, Creighton University, Omaha, NE, USA

Abstract

Behavioral and neural responses to visual scenes depicting potential threat or harm constitute core aspects of human behavior and can illuminate symptoms of internalizing disorders. Decades of research have shown that negative content undergoes facilitated processing across a distributed brain network whereby perception is facilitated, and cognitive systems appraise the stimulus to regulate emotions and plan motor action. However, relatively limited studies have examined the multispectral dynamics underlying the neural processing of negative emotional images, with mixed results among existing studies. Herein, we used magnetoencephalography (MEG) to derive dynamic functional maps of positive and negative image processing in healthy adults. Alpha (from 200 to 700 ms) and beta (from 200 to 550 ms) oscillations were stronger for negative images in primary and ventral visual regions, as well as parietal and prefrontal cortices (all $ps < .005$). Similarly, theta activation was stronger for negative images in ventral temporal cortex ($p < .001$) from 0 to 250 ms. Lastly, gamma oscillatory activity was stronger for negative images in the pre-supplementary motor area ($p < .005$) from 150 to 500 ms. These results are consistent with the literature in regard to the critical brain regions involved in emotional processing, but importantly also delineate the multispectral oscillatory dynamics within these regions that support the swift synthesis of low-level visual inputs, appraise emotional meaning, and guide appropriate motor system activation (as necessary) to avoid harm.

*Corresponding author. nathan.petro@boystown.org (N.M. Petro).

CRediT authorship contribution statement

Nathan M. Petro: Writing – review & editing, Writing – original draft, Visualization, Software, Formal analysis. **Mikki Schantell:** Supervision, Formal analysis, Conceptualization. **Mia C. Lulli:** Formal analysis, Data curation. **Kellen M. McDonald:** Formal analysis. **Chloe C. Casagrande:** Software, Methodology. **Christine M. Embury:** Software, Methodology. **Hannah J. Okelberry:** Project administration, Investigation. **Jason A. John:** Project administration, Investigation. **Ryan Glesinger:** Project administration, Investigation. **Lucy K. Horne:** Project administration, Investigation. **Giorgia Picci:** Writing – review & editing. **Tony W. Wilson:** Writing – review & editing, Supervision, Resources, Project administration, Methodology, Investigation, Funding acquisition, Conceptualization.

Declaration of competing interest

All authors report no biomedical financial interests or potential conflicts of interest.

Keywords

Emotion; Magnetoencephalography; MEG; Theta; Gamma; Alpha

1. Introduction

To help ensure survival, complex organisms must successfully respond to sensory information conveying potential threat or harm (Konorski, 1967; Schneirla, 1959). In the laboratory, one method to study responses to threat is to present images that depict negative information relevant to physical harm and/or survival (e.g., a weapon, a dangerous animal; Lang et al., 1997b). Nearly a century of research has demonstrated that such negative images prompt a cascade of physiological reactions (e.g., changes in heart rate, respiration, pupil dilation; (Bradley and Lang, 2000; Lang and Bradley, 2013; Öhman and Wiens, 2003)) that aid perception (Campbell et al., 1997; Fanselow, 1994) and support a disposition toward necessary action (Frijda, 2000; Lang et al., 1990; Öhman et al., 2001). Conversely, atypically strong responses to negative information (i.e., a negativity bias) are a transdiagnostic hallmark of anxiety and mood disorders (Lang et al., 2016; McTeague and Lang, 2012). Thus, characterizing the neurophysiology involved in processing negative information is critical to understanding not only a core feature of human behavior, but also symptoms of mental health disorders.

Decades of neuroimaging have shown that responses to negative emotional stimuli involve widespread brain regions, implicating many aspects of human behavior and psychology. Multiple meta-analyses and reviews have shown that some of the most consistent brain responses to emotional pictures occur in the ventral occipitotemporal cortices, extending into the amygdalae, prefrontal and inferior frontal cortices, the anterior cingulate, and the insula (Kober et al., 2008; Lindquist et al., 2012; Sabatinelli et al., 2011; Stevens and Hamann, 2012; Wager et al., 2015). Activation of the ventral visual regions reflects the processing of sensory information along the visual hierarchy (Grill-Spector et al., 2001; Iordan et al., 2015; Kiani et al., 2007), where its emotional meaning is extracted (Sabatinelli and Frank, 2019; Taylor et al., 2000) and sensory representation enhanced through re-entrant connections (Keil et al., 2009; Vuilleumier, 2005). Activation within frontal cortices is likely indicative of cognitive processes (Barrett, 2017; Ochsner and Gross, 2005) which appraise and elaborate upon (Lang and Bradley, 2010) the negative information to create appropriate behavioral programs to avoid harm (Adolphs, 2003; Frijda, 2000). Particularly in the context of negative images, such frontal cortical activity is thought to reflect higher-order processes of emotion regulation (Buhle et al., 2014; Domes et al., 2010; Ochsner and Gross, 2005), where individual differences reflect tendencies toward or away from a negativity bias (Petro et al., 2018, 2021; Urry, 2006). The broad consensus from neuroimaging is that negative information activates multiple brain networks to facilitate perception and attention, as well as higher-order processes to assess and plan appropriate action.

Brain activity measured by electroencephalography (EEG) have also been used to study negative image processing, particularly the neural dynamics which can enable multispectral (e.g., theta, gamma, etc.) analyses of neural oscillatory activity supporting various features

of visual perceptual, attention, and higher-order cognitive processes. In this context, stronger gamma frequency responses have been observed for negative compared to neutral and/or positive images (Balconi et al., 2009a; Balconi and Lucchiari, 2006; Keil et al., 2001, 2007; Martini et al., 2012; Müller et al., 1999; Sato et al., 2011), thought to reflect efficient, facilitated processing of the biologically relevant negative stimuli. Studies of theta oscillations in response to negative emotional stimuli are more limited, with the available evidence suggesting stronger frontal theta responses for negative compared to neutral (Zhang et al., 2012) and positive images (Balconi et al., 2009a; Knyazev et al., 2010), although others have found equal responses for negative and positive with both being stronger than neutral (Balconi et al., 2009b; Knyazev et al., 2009). Thus, while negative images tend to elicit stronger responses than neutral, the differences between negative and positive images have been inconsistent across studies.

Similar effects have been observed for alpha and beta responses, but the extent to which these effects are unique to negative images is unclear. Stronger alpha and beta oscillations (i.e., greater decreases from baseline, or desynchronizations) have long been tied to visual attention function (Klimesch, 2012; Ray and Cole, 1985; Wiesman et al., 2017), and are thought to reflect active cortical engagement (Pfurtscheller and Klimesch, 1992). Multiple studies have shown that stronger oscillations for negative compared to neutral images in alpha (Balconi et al., 2009a; Cui et al., 2013; De Cesarei and Codispoti, 2011; Ferrari et al., 2015, 2022; Friedl and Keil, 2021; Huster et al., 2009; Messerotti Benvenuti et al., 2019; Murphy et al., 2020; Panitz et al., 2019; Simons et al., 2003; Sollfrank et al., 2021; Wang et al., 2021) and beta (Meng et al., 2016; Schubring et al., 2020), suggesting that negative emotional content engages attention systems in a bottom-up fashion. Some of these studies have reported similar effects in response to positive and neutral images for alpha (Balconi et al., 2009a; Cui et al., 2013; De Cesarei and Codispoti, 2011; Ferrari et al., 2015, 2022; Messerotti Benvenuti et al., 2019; Murphy et al., 2020; Simons et al., 2003; Wang et al., 2021) and beta (Schubring et al., 2020; Schubring and Schupp, 2019, 2021), while others have found stronger oscillations for negative compared to positive images (Huster et al., 2009; Keil et al., 2001; Luther et al., 2023). There are also a collection of studies that have reported no difference between positive or negative from neutral in alpha (Aftanas et al., 2001; Arana et al., 2022; Dell'Acqua et al., 2022; Lee et al., 2017) and beta (Müller et al., 1999; Noguchi and Kubo, 2020). These mixed results may be due to inconsistencies in the arousal levels of different categories of images, different task parameters imposed during the viewing of the images, and/or different strategies of electrode-level EEG data analyses (Codispoti et al., 2023; Güntekin and Basar, 2007). Establishing whether alpha/beta oscillations to emotional images are stronger for negative compared to positive images, and the precise brain regions contributing to these differences would provide critical advances in the study of negativity bias in anxiety and mood disorders. The limited studies that have used magnetoencephalography (MEG) source imaging during emotional stimulus processing have focused on the gamma-band (Luo et al., 2007, 2009).

The current study aimed to map the spatiotemporal oscillatory dynamics underlying the processing of negative emotional images. Given our goals of identifying the precise brain regions involved, we quantified the neurophysiological activity using MEG while individuals viewed arousal-matched negative and positive images. Negative and positive,

rather than low-arousing neutral, images were compared to highlight brain responses related to negative emotional content rather than that related to high versus low arousing content. The MEG recordings were imaged in the time-frequency domain using a whole-brain beamformer source reconstruction approach and submitted to a voxel-wise paired-samples *t*-test. We hypothesized that negative compared to positive images would elicit stronger neural oscillations in the alpha and beta bands in frontoparietal attention regions, as well as stronger theta and gamma oscillations in association cortices that support emotional processing.

2. Methods

2.1. Participants

We enrolled a relatively homogeneous sample to minimize the impact of cultural differences on emotional image processing. Specifically, we enrolled a total of 36 right-handed, young adults (21 females) with a mean age of 27.64 (SD = 4.04; range: 21.35–35.12) who were generally highly educated for their age (mean education level: 16.61 years). The sample was 5.56 % Black, 2.78 % American Indian/Alaska Native, 13.89 % Asian, 75.00 % Caucasian, and 2.78 % more than one race. This distribution corresponds to the racial demographics of the surrounding area. Exclusionary criteria included any medical illness affecting CNS function (e.g., HIV/AIDS, Lupus, etc.), a current or past diagnosis of any neurological or psychiatric disorder by a medical professional, history of head trauma, current substance abuse, and the standard exclusionary criteria related to MEG and MRI acquisition (e.g., ferromagnetic implants). The Boys Town National Research Hospital's Institutional Review Board reviewed and approved this investigation. Each participant provided written informed consent following a detailed description of the study.

2.2. Experimental paradigm

During the MEG recording, participants sat in a nonmagnetic chair within a magnetically shielded room. All stimuli were presented using the Psychophysics Toolbox (Kleiner et al., 2007) and a PROPixx DLP LED projector (VPixx Technologies Inc., Saint-Bruno-de-Montarville, Canada). The experiment consisted of 220 trials. In each trial, a fixation cross appeared for a duration of 1000 to 1400 ms and this was replaced by a picture that was presented centrally for 1800 ms (Fig. 1). Stimuli consisted of 100 pleasant and 100 unpleasant images. Of these 200 images, 44 images were selected from the International Affective Picture System (IAPS; (Lang et al., 1997a)) and 154 from the Nencki Affective Picture System (NAPS; (Marchewka et al., 2013)). All stimuli were 560 × 420 pixels in size. The valence ratings confirmed that positive (M = 6.58, SD = 0.82) images were rated as more positive than negative (M = 3.86, SD = 0.84) images (t_{198} = 23.17, p < .001). Importantly, the arousal rating did not differ (t_{198} = −1.45, p > .05) between the positive (M = 3.49, SD = 1.06) and negative (M = 3.71, SD = 1.12) images. Each of the negative and positive image groups were comprised of 25 landscapes, 25 animals, 25 common objects, and 25 people. Lastly, negative and positive images did not differ based on luminance (t_{198} = 0.32, p > .05) or contrast (t_{198} = 0.82, p > .05), and did not differ in any spatial frequency (all ps > 0.05).

To ensure participants paid attention, 20 oddball images of musical instruments were presented pseudo-randomly and participants were instructed to respond via button press. All participants responded to at least 75 % of the oddball stimuli, and all oddball trials were excluded from subsequent analysis. None of the standard trial images contained musical instruments. Stimuli were presented in a pseudo-randomized order such that the valence (positive or negative) nor category (landscape, animal, common objects, or people) were repeated in more than three consecutive trials.

2.3. MEG and MRI data acquisition

All MEG recordings were conducted in a two-layer magnetically-shielded VACOSHIELD room (Vacuumschmelze, Hanau, Germany). Neuromagnetic responses were sampled continuously at 1 kHz, with an acquisition bandwidth of 0.1–330 Hz, using a MEGIN Triux Neo MEG system with 306 magnetic sensors (Helsinki, Finland). During data acquisition, participants were monitored via real-time audio-visual feeds from inside the shielded room. Participant-wise MEG data were corrected for head motion and subjected to external noise reduction using the signal space separation method with a temporal extension (Taulu and Simola, 2006; Uutela et al., 2001). High-resolution structural images were collected using a 1-mm isotropic MPRAGE sequence [TR = 2.3 s, TE = 2.98 ms, flip angle = 9°, FOV = 256 mm] on a Siemens Prisma 3-T scanner with a 64-channel head coil.

2.4. Structural MRI processing and MEG coregistration

Preceding MEG measurement, five head position indicator (HPI) coils were attached to the participant's head and localized, together with three fiducial points and at least 100 scalp surface points, with a 3D digitizer (Fastrak, Polhemus Navigator Sciences, Colchester, VT, USA). Once in the MEG, electrical currents of unique frequencies (e.g., 322 Hz) were fed into each of the HPI coils, which induced measurable magnetic fields, allowing the position of the coils to be actively tracked relative to the MEG sensors throughout the recording. Since the HPI coil locations were also known in head coordinates, all MEG measurements could be transformed into a common coordinate system. With this coordinate system, participant-wise MEG data were coregistered with the participant's high-resolution structural T1-weighted MRI data prior to source reconstruction using BESA MRI (Version 3.0, BESA GmbH, Gräfelfing, Germany). Structural MRI data were aligned parallel to the anterior and posterior commissures and transformed into standardized space. Following source reconstruction (i.e., imaging), each participant's MEG functional images were also transformed into standardized space and spatially resampled to enable statistical comparisons across participants.

2.5. MEG preprocessing, time-frequency transformation, and sensor-level statistics

Cardiac and ocular artifacts (blinks and eye movements) were removed from the data using signal-space projection (SSP), which was accounted for during source analysis (Uusitalo and Ilmoniemi, 1997). The continuous magnetic time series was divided into 1800 ms epochs (−600 to 1200 ms), with stimulus onset defined as 0 ms and the baseline period being defined as the 500 ms prior to image onset (i.e., −500 to 0 ms). Subsequently, epochs with remaining artifacts were removed based on a fixed threshold method, supplemented with visual inspection.

Briefly, the MEG raw signal amplitude is strongly affected by distance between the brain and the MEG sensor array, as the magnetic field strength sharply falls off as the distance from the source current increases. Thus, the average amplitude of cortical activity recorded by the MEG sensor array will vary as a function of individual head size and position within the MEG bore. To account for this source of variance across participants, as well as actual variance in neural response amplitude, rejection of artifactual trials was determined using the amplitude and gradient distributions across all trials were determined per participant based on the individual distribution of signal amplitude and gradient. Trials containing the highest amplitude and/or gradient values relative to this distribution were rejected based on participant-specific thresholds. Across all participants, the average amplitude threshold was 1115.69 (SD = 392.44) fT/cm and the average gradient threshold was 212.92 (SD = 112.92) fT/(cm × ms). Following artifact rejection, an average of 91.92 (SD = 4.33) negative and 93.00 (SD = 5.25) positive condition trials were included in the final analysis. The number of trials did not statistically differ by condition ($p > .05$; see Results).

Artifact-free epochs were then transformed into the time-frequency domain using complex demodulation (Kovach and Gander, 2016), with a resolution of 2 Hz and 25 ms between 4 and 100 Hz. Following time-frequency transformation, spectral power estimates per sensor were averaged across trials to generate plots of mean spectral density per sensor. These sensor-level data were then normalized using the baseline power within each frequency bin, which was calculated as the mean power for that 2.0 Hz bin during the −500 to 0 ms baseline period. The significant time-frequency windows used for source imaging were then determined by statistical analysis of the sensor-level spectrograms across the entire array of 204 gradiometers, which was conducted in BESA Statistics (Version 2.1T, BESA GmbH, Gräfelfing, Germany). Briefly, each pixel per spectrogram was initially evaluated using a mass univariate approach based on the general linear model, followed by cluster-based permutation testing to address the problem of multiple comparisons (Ernst, 2004; Maris and Oostenveld, 2007). This two-stage procedure was utilized to minimize false positive results while maintaining sensitivity, with the first stage consisting of paired-sample *t*-tests against baseline on each pixel per spectrogram and thresholding the output spectrograms of *t*-values at $p < .05$ to define time-frequency bins containing potentially significant oscillatory responses. In stage two, the time-frequency bins that survived thresholding (at $p < .05$) were clustered with temporally and/or spectrally neighboring bins that also survived, and cluster values were derived by summing all *t*-values within each cluster. Nonparametric permutation testing was then used to derive a distribution of cluster values and the significance level of the cluster(s) were tested directly using this permuted distribution, which was the result of 10,000 permutations. Based on this cluster-based permutation analysis, only the time-frequency windows that contained significant oscillatory deviations from baseline at the $p < .001$, corrected, threshold across all participants were subjected to source imaging (i.e., beamforming).

2.6. MEG source imaging

Cortical regions were imaged through a time-frequency-resolved extension of the linearly constrained minimum variance (LCMV) beamformer (Dalal et al., 2006; Gross et al., 2001; Van Veen et al., 1997), with a single shell volume conductor and regularization

based on singular value decomposition (SVD) at 0.0001 %. The images were derived from the cross spectral densities of all combinations of MEG gradiometers averaged over the time-frequency range of interest, and the solution of the forward problem for each location on a grid specified by input voxel space (4 × 4 × 4 mm voxels). In principle, the beamformer operator generates a spatial filter for each grid point that passes signals without attenuation from a given neural region, while suppressing activity in all other brain areas. The filter properties arise from the forward solution (i.e., lead field matrix) for each location on a volumetric grid specified by input voxel space, and from the MEG cross spectral density matrix. Basically, for each voxel, a set of beamformer weights is determined, which amounts to each MEG sensor being allocated a sensitivity weighting for activity in that particular voxel. Following convention, the source power in these images was normalized per participant using a pre-stimulus period (i.e., baseline) of equal duration and bandwidth (Hillebrand et al., 2005). Such images are typically referred to as pseudo-*t* maps, with units (pseudo-*t*) that reflect noise-normalized power differences (i.e., active vs. passive) per voxel. MEG pre-processing and imaging used the Brain Electrical Source Analysis (version 7.1) software. Individual participant-level maps were examined to reject images containing clear artifacts (e.g., striping or “ribboning”) or extreme values across the brain. This procedure was conducted separately for each time-frequency window, and those containing significant artifacts were excluded from further analysis.

2.7. Whole-brain statistics

To identify differences in neural oscillatory power as a function of image valence, the whole-brain voxel-wise maps per oscillatory response were projected through a gray matter mask and examined using paired-samples *t*-tests (two-tailed), computed in MATLAB. To account for multiple comparisons, a cluster forming threshold of $p < .005$ and cluster-extent threshold of $k > 10$ (i.e., > 640 mm^3) were used, based on Gaussian random fields theory (Poline et al., 1995; Worsley et al., 1996).

3. Results

Participants performed well on the oddball task, with a mean accuracy rate of 95 % (SD = 7.27 %; range = 75–100 %) and mean reaction time of 765 ms (SD = 114 ms; range = 559–1122 ms). Following artifact rejection and exclusion of incorrect trials, each participant had an average of 91.92 (SD = 4.33) and 93.00 (SD = 5.25) trials in the negative and positive conditions, respectively, for beamforming. The number of retained trials did not differ between conditions ($t_{35} = 1.61$, $p > .05$).

3.1. Sensor-level neural responses

Statistical analysis of the sensor-level spectrograms using our two-stage nonparametric permutation testing approach (see Section 2.6) revealed clusters of sustained power decreases relative to baseline in the alpha (10–16 Hz) range from 200 to 700 ms and in the beta (20–26 Hz) band from 200 to 550 ms ($p < .001$, corrected; Fig. 2). These time windows were imaged using baselines of equal bandwidth and duration (alpha: −500 to 0 ms; beta: −500 to −150 ms), which is essential to ensure amplitudes in the beamformer images are not biased by differing numbers of datapoints (Singh et al., 2002). In addition, there were

increases in power from baseline in the theta (4–8 Hz) band from 50 to 300 ms and in the gamma (62–92 Hz) range from 150 to 500 ms following stimulus onset ($p < .001$, corrected; Fig. 2). These two time-windows were imaged using baselines of −500 to −250 ms and −500 to −150 ms, respectively. Following imaging, each oscillatory response was grand-averaged across all participants and conditions to visualize the brain regions generating the strongest responses. Rejection of artifactual images resulted in the removal of four participants for theta, three for alpha, two for beta, and two for gamma.

3.2. Functional mapping of oscillatory responses

The oscillatory maps for negative and positive conditions were submitted to voxel-wise paired samples *t*-tests (two-tailed; see Section 2.8). These tests revealed significantly stronger responses for negative compared to positive conditions in the theta, alpha, beta, and gamma frequency bands. In contrast, no regions exhibited significantly stronger oscillatory responses during positive compared to negative images. The MNI coordinates and cluster sizes are listed in Table 1.

In the alpha- and beta-bands, stronger oscillations (i.e., decreases from baseline, or desynchronizations) were observed for negative compared to positive images across seven and six clusters, respectively. Alpha oscillations were stronger during negative image processing in the left temporoparietal junction (TPJ; $t_{32} = -4.79$, $p < .001$, Cohen's d = 0.83), the right inferior occipital gyrus ($t_{32} = -3.97$, $p < .001$, Cohen's d = 0.69), the right superior frontal gyrus ($t_{32} = -3.90$, $p < .001$, Cohen's d = 0.68), the left middle occipital gyrus ($t_{32} = -3.53$, $p < .005$, Cohen's d = 0.61), the right superior parietal lobule ($t_{32} = -3.50$, $p < .005$, Cohen's d = 0.61), left cerebellum ($t_{32} = -3.48$, $p < .005$, Cohen's d = 0.61), and the right middle occipital gyrus ($t_{32} = -3.41$, $p < .005$, Cohen's d = 0.59; Fig. 3). Beta oscillations were stronger during negative images in the left inferior frontal gyrus (extending into the middle frontal gyrus and the superior insula; $t_{33} = -5.31$, $p < .001$, Cohen's d = 0.91), in the left inferior temporal cortex ($t_{33} = -4.63$, $p < .001$, Cohen's d = 0.79), the right inferior parietal cortex ($t_{33} = -4.46$, $p < .001$, Cohen's d = 0.76), a posterior portion of the left cerebellum ($t_{33} = -3.84$, $p < .001$, Cohen's d = 0.66), an anterior portion of the left cerebellum ($t_{33} = -3.39$, $p < .005$, Cohen's d = 0.58), and the right middle cingulate gyrus ($t_{33} = -3.18$, $p < .005$, Cohen's d = 0.55).

In the theta-band, neural oscillations were stronger for negative ($t_{31} = 4.27$, $p < .001$, Cohen's d = 0.75; Fig. 4) images in one cluster that included the left parahippocampal gyrus and inferior temporal lobe. Gamma activity was also stronger for negative compared to positive images in four clusters, including the right intraparietal sulcus ($t_{33} = 3.66$, $p < .001$, Cohen's d = 0.63), right posterior hippocampus ($t_{33} = 3.58$, $p < .005$, Cohen's d = 0.61), right supplemental motor area ($t_{33} = 3.42$, $p < .005$, Cohen's d = 0.59) and the right posterior cingulate cortex ($t_{33} = 3.39$, $p < .005$, Cohen's d = 0.59; Fig. 4). Lastly, no brain regions showed stronger neural oscillations in any band during positive relative negative image processing.

4. Discussion

We identified stronger neural oscillations for negative compared to positive images in an early theta (50 to 300 ms) window and more extended gamma (150 to 500 ms) window, and temporally overlapping periods with stronger (i.e., more negative) alpha (200 to 700 ms) and beta (200 to 550 ms) oscillations. The location of these effects are consistent with multiple meta-analyses (Kober et al., 2008; Lindquist et al., 2012; Sabatinelli et al., 2011), where emotional picture processing involves both low- and high-level visual processing within primary occipital, ventral visual, and parietal cortices, as well as higher-order cognitive regions which appraise the emotional content and plan subsequent action. In sum, the results indicate that negative images more strongly engage widespread brain regions reflecting heightened perceptual processing and preparation for mobilization.

Theta activity immediately following stimulus onset (50 to 300 ms) was stronger for negative compared to positive images within the inferior temporal cortex, consistent with findings indicating that theta is typically strongest for negative images (Aftanas et al., 2002; Balconi et al., 2009b, 2009a) or facial expressions (Balconi and Lucchiari, 2006; Knyazev et al., 2009, 2010; Zhang et al., 2012). Similar theta effects point to its role in guiding visual attention (Meehan et al., 2021; Wiesman et al., 2017, 2018; Wiesman and Wilson, 2019). While theta activity is related to numerous aspects of cognition (Cavanagh and Frank, 2014), the relatively early timing suggests this effect reflects visual processing. In fact, the timing of this effect is also consistent with ERP results (Hinojosa et al., 2015; Schindler and Bublatzky, 2020) which have been used as evidence that rapid visual processes prioritize the emotional information. Along these lines, theta differences within the ventral visual pathway and inferior temporal cortex are broadly consistent with studies of emotional picture processing (Sabatinelli et al., 2011; Sabatinelli and Frank, 2019) and these regions are known to be critically involved in high-tier visual processing (Kiani et al., 2007). Taken together, these theta differences likely reflect the rapid and efficient visual processing of motivationally relevant information conveyed by the negative arousing pictures.

Stronger alpha and beta oscillations (i.e., decreases relative to baseline, or desynchronizations) for negative relative to positive images were observed in multiple visual and attention regions. Such alpha and beta oscillations have long been associated with active cortical engagement (Pfurtscheller and Klimesch, 1992), often during states of top-down visual attention (Klimesch, 2012; Petro et al., 2019; Petro and Keil, 2015; Wiesman et al., 2017) and/or during active working memory (Hanslmayr et al., 2012; Heinrichs-Graham and Wilson, 2015; Pavlov and Kotchoubey, 2022; Proskovec et al., 2016, 2019; Springer et al., 2023). While negative images have consistently been linked to stronger alpha/beta responses (Balconi et al., 2009a; Cui et al., 2013; De Cesarei and Codispoti, 2011; Ferrari et al., 2015, 2022; Friedl and Keil, 2021; Huster et al., 2009; Messerotti Benvenuti et al., 2019; Murphy et al., 2020; Panitz et al., 2019; Schubring et al., 2020; Sollfrank et al., 2021; Wang et al., 2021), mixed results have been observed in regards to positive images (Balconi et al., 2009a; Cui et al., 2013; De Cesarei and Codispoti, 2011; Ferrari et al., 2015, 2022; Huster et al., 2009; Keil et al., 2001; Messerotti Benvenuti et al., 2019; Murphy et al., 2020; Schubring et al., 2020; Schubring and Schupp, 2019, 2021; Wang et al., 2021; see Codispoti et al., 2023; Güntekin and Basar, 2007 for reviews). These inconsistencies may reflect analytical

differences or perhaps differential mixing of sources due to volume conduction, as the vast majority of studies in this area have not utilized source imaging. The current results indicate that negative compared to positive images elicit stronger alpha/beta oscillations, at least within frontal and parietal cortices. Moreover, these results suggest that negative images engage neural regions integral to facilitating attention and memory processes more strongly.

Along these lines, these alpha and beta effects were predominantly located across several canonical attention and higher-order cognitive regions. Alpha and beta responses were stronger in ventral occipital and temporal cortices, where low-level visual information is synthesized into coherent percepts (Grill-Spector et al., 2001; Iordan et al., 2015; Kiani et al., 2007) capable of conveying emotional meaning (Sabatinelli and Frank, 2019; Taylor et al., 2000). Alpha and beta responses were also stronger in nearby inferior parietal regions, known to be critical to top-down visual attention (Arif et al., 2022; Corbetta and Shulman, 2002; Liu et al., 2016). Alpha oscillations were also stronger for negative pictures in the TPJ, which is implicated in domain-general cognitive function (Igelström and Graziano, 2017) and global scene perception (Rennig et al., 2024). Moreover, this region plays a key role in guiding attention toward emotional information (Inuggi et al., 2014; Kastner et al., 2017; Kim et al., 2018) and determining its emotional relevance (Patel et al., 2019; Schurz et al., 2014). Alpha was also stronger for negative images in primary visual cortex. Thus, our alpha and beta results are consistent with prior works, suggesting emotional processing engages high-tier visual, attention, and higher-order cognitive processes (Kober et al., 2008), but also the involvement of low-level sensory cortex in emotion processing (Bradley et al., 2003; Li and Keil, 2023).

Alpha and beta oscillations were also observed in frontal cortices implicated in emotion regulation. For example, alpha responses were stronger for arousing images in the superior frontal cortex, a region frequently implicated in cognitive reappraisal of emotional information (Kober et al., 2008; Lindquist et al., 2012) and the generation of emotional imagery (Diekhof et al., 2011) that is necessary for successful emotion regulation (Buhle et al., 2014; Domes et al., 2010; Petro et al., 2018). The same effect was present for beta in the inferior frontal cortex extending into the insula, regions also observed during emotion regulation (Grecucci et al., 2013; Jabbi and Keysers, 2008; Petro et al., 2018). Notably, the insula is also thought to be involved in changes in physiological states during emotional arousal (Kober et al., 2008; Zaki et al., 2012). Together, the patterns of stronger alpha and beta oscillations during negative images involved brain regions that underlie the appraisal of emotional information and are thought to be central to emotion regulation. It should be noted, however, participants freely viewed the images in this study and were not given explicit instructions to appraise the images or regulate emotional responses. Thus, caution is warranted and future work should directly test this interpretation by implementing paradigms that require appraisal of images and/or emotion regulation.

We also observed stronger gamma oscillations during negative compared to positive images in multiple brain regions, including the pre-SMA. Stronger gamma activation has been observed for emotional relative to neutral images (Keil et al., 2001, 2007; Martini et al., 2012; Müller et al., 1999) and for negative compared to neutral and/or positive facial expressions (Balconi and Bortolotti, 2013; Luo et al., 2007, 2009; Sato et al., 2011). In

fact, a recent finding from our laboratory found stronger gamma for negative compared to neutral and positive facial expressions within the same pre-SMA region (Petro et al., 2025). More broadly, this pre-SMA region has been implicated in emotional processing in general (Kober et al., 2008; V. I. Müller et al., 2018; Sabatinelli et al., 2011). Increased pre-SMA gamma has been observed immediately preceding target-directed motor movement (Gaetz et al., 2013; Gunduz et al., 2016). Thus, the current findings are consistent with observed changes in motor action preparation circuitry during emotional picture processing (Borgomaneri et al., 2015; Bradley et al., 2001; Coombes et al., 2005; Pitcher et al., 2008), and more broadly the long-held notion that motor system activation is a fundamental component of emotion processing (Frijda, 2000; Lang and Bradley, 2010). In addition, gamma oscillatory activity was stronger during negative compared to positive images in the posterior hippocampus, which is strongly tied to many aspects of memory (Squire et al., 2001), in particular the high-tier visual processing involved in memory retrieval (Fanselow and Dong, 2010; Grady, 2020). This effect was present also in the intraparietal and posterior cingulate cortices, which serve similar functions related to visual attention (Arif et al., 2022; Proskovec et al., 2018), imagery (Leech and Sharp, 2014), and cognition (Foster et al., 2022). These effects in the gamma band thus reflect multiple processes extending from sensory information processing to memory and recognition to motor action planning based on output assessments.

Before closing, it is important to acknowledge limitations of this study. First, no neutral images were used. Instead, only arousal-matched pleasant and unpleasant images were used to focus on the effect of negative images, given that negativity bias is a transdiagnostic feature of anxiety and mood disorders. Future work should test if these results extend to comparisons with low-arousing neutral images. One possibility is that erotic images, often included in studies of positive image processing, would likely produce similar levels of alpha and beta responses (Schubring and Schupp, 2021). Erotic images were not included in the current study given our long-term goal of extending this task to adolescents and the ethical considerations that come into play with younger populations. Along these lines, future studies should test if these findings extend to younger and older populations given the known protracted developmental course of affective and complex visual processing (Dilks et al., 2022; Herba et al., 2006). Moreover, individual differences related to mental health symptoms, particularly internalizing symptoms, as well as those with diagnosed mental illness, should also be examined given that changes in emotion image processing are known to occur (Gentili et al., 2016; MacNamara et al., 2017; Marwick and Hall, 2008; Pei et al., 2023). Next, participants were all young adults and highly educated, with a fairly homogenous demographic profile to limit individual variability of arousal responses to the images (Roberts and Levenson, 2006). This homogeneity does however limit the generalizability of our findings. Further, we relied on self-report questionnaires to determine that our enrollees did not have current or past diagnoses of psychiatric or neurological conditions, and future studies should consider implementing psychiatric and cognitive assessments as part of the enrollment process. Lastly, MEG inherently has reduced sensitivity to deeper sources (Hillebrand and Barnes, 2002) such as the amygdala. Thus, it is possible that amygdala activity may not have been detected in the current study. However, we note that many studies have shown that MEG systems like that used in the current

study are sensitive enough to detect neural activity in the hippocampal area, amygdala, and neighboring regions (Badura-Brack et al., 2017; Badura-Brack, McDermott, Becker, et al., 2018; Badura-Brack, McDermott, Heinrichs-Graham, et al., 2018; Lew et al., 2021; Meehan et al., 2021; Ott et al., 2021; Petro et al., 2022; Picci et al., 2023; Rempe et al., 2025), and the current results showed stronger hippocampal gamma for negative compared to positive images, which agrees with past work as reviewed above. Nonetheless, future work in this area should consider multimodal approaches to ensure full sensitivity to deeper sources.

The current study found stronger theta, alpha, beta, and gamma oscillations during negative compared to positive image processing across widespread brain regions, whose function ranges from low-level visual processing in primary visual cortex, to image formation and visual attention in extended visuocortical and parietal regions, to higher-order cognitive processes in frontal cortices that likely underlie emotion regulation. This cortical hierarchy of negative image processing is consistent with models proposed in prior works (Du et al., 2023; Vuilleumier and Pourtois, 2007). Broadly, in the context of prior literature on the function of these frequency bands, the stronger responses toward negative compared to positive images in visuocortical alpha likely reflect the engagement of attention, while that in parietal and pre-SMA cortical gamma reflect the integration of visual information which may inform future motor action. These results are consistent with the notion that the processing of negative images is a multifaceted process involving the identification of emotionally relevant sensory information in ventral visual and temporal regions, the facilitation of attention toward emotional content, and the higher-order cognitive processes necessary to successfully appraise the negative, potentially threatening information and initiate strategic behavioral programs (Adolphs, 2003). This investigation highlights the utility of multispectral dynamic imaging in the context of multistage emotional processing, which may illuminate the neural bases of emotional dysregulation in mental health disorders.

Funding acknowledgments

This study was supported by the National Institutes of Health through grants R01-MH116782 (TWW), S10-OD028751 (TWW), R01-MH118013 (TWW), R01-DA056223 (TWW), R01-DA059877 (TWW), and P20-GM144641 (GP and TWW). The funders had no role in the study design, collection, analysis, or interpretation of data, nor did they influence writing the report or the decision to submit this work for publication.

Data availability

The data used in this article will be made publicly available through the COINS framework at the completion of the study (https://coins.trendscenter.org/).

References

Adolphs R, 2003. Cognitive neuroscience of human social behaviour. Nature Rev. Neurosci. 4 (3). 10.1038/nrn1056. Article 3.

Aftanas LI, Varlamov AA, Pavlov SV, Makhnev VP, Reva NV, 2002. Time-dependent cortical asymmetries induced by emotional arousal: EEG analysis of event-related synchronization and desynchronization in individually defined frequency bands. Int. J. Psychophysiol. 44 (1), 67–82. 10.1016/S0167-8760(01)00194-5. [PubMed: 11852158]

Aftanas LI, Varlamov A, Pavlov S, Makhnev V, Reva N, 2001. Event-related synchronization and desynchronization during affective processing: emergence of valence-related time-dependent hemispheric asymmetries in theta and upper alpha band. Int. J. Neurosci. 110 (3–4), 197–219. 10.3109/00207450108986547. [PubMed: 11912870]

Arana L, Melcón M, Kessel D, Hoyos S, Albert J, Carretié L, Capilla A, 2022. Suppression of alpha-band power underlies exogenous attention to emotional distractors. Psychophysiology. 59 (9), e14051. 10.1111/psyp.14051.

Arif Y, Embury CM, Spooner RK, Okelberry HJ, Willett MP, Eastman JA, Wilson TW, 2022. High-definition transcranial direct current stimulation of the occipital cortices induces polarity dependent effects within the brain regions serving attentional reorientation. Hum. Brain Mapp. 43 (6), 1930–1940. 10.1002/hbm.25764. [PubMed: 34997673]

Badura-Brack A, Heinrichs-Graham E, McDermott TJ, Becker KM, Ryan TJ, Khanna MM, Wilson TW, 2017. Resting-State neurophysiological abnormalities in Posttraumatic Stress disorder: A magnetoencephalography study. Front. Hum. Neurosci. 11, 205. 10.3389/fnhum.2017.00205. [PubMed: 28487642]

Badura-Brack A, McDermott TJ, Becker KM, Ryan TJ, Khanna MM, Pine DS, Bar-Haim Y, Heinrichs-Graham E, Wilson TW, 2018a. Attention training modulates resting-state neurophysiological abnormalities in posttraumatic stress disorder. Psychiatry Res. Neuroimag. 271, 135–141. 10.1016/j.pscychresns.2017.11.008.

Badura-Brack A, McDermott TJ, Heinrichs-Graham E, Ryan TJ, Khanna MM, Pine DS, Bar-Haim Y, Wilson TW, 2018b. Veterans with PTSD demonstrate amygdala hyperactivity while viewing threatening faces: A MEG study. Biol. Psychol. 132, 228–232. 10.1016/j.biopsycho.2018.01.005. [PubMed: 29309826]

Balconi M, Bortolotti A, 2013. Conscious and unconscious face recognition is improved by high-frequency rTMS on pre-motor cortex. Conscious. Cogn. 22 (3), 771–778. 10.1016/j.concog.2013.04.013. [PubMed: 23727711]

Balconi M, Brambilla E, Falbo L, 2009a. Appetitive vs. Defensive responses to emotional cues. Autonomic measures and brain oscillation modulation. Brain Res. 1296, 72–84. 10.1016/j.brainres.2009.08.056. [PubMed: 19703433]

Balconi M, Brambilla E, Falbo L, 2009b. BIS/BAS, cortical oscillations and coherence in response to emotional cues. Brain Res. Bull. 80, 151–157. 10.1016/j.brainresbull.2009.07.001. [PubMed: 19591907]

Balconi M, Lucchiari C, 2006. EEG correlates (event-related desynchronization) of emotional face elaboration: A temporal analysis. Neurosci. Lett. 392 (1), 118–123. 10.1016/j.neulet.2005.09.004. [PubMed: 16202519]

Barrett LF, 2017. The theory of constructed emotion: an active inference account of interoception and categorization. Soc. Cogn. Affect. Neurosci. 12 (1), 1–23. 10.1093/scan/nsw154. [PubMed: 27798257]

Borgomaneri S, Vitale F, Avenanti A, 2015. Early changes in corticospinal excitability when seeing fearful body expressions. Sci. Rep. 5 (1), 14122. 10.1038/srep14122. [PubMed: 26388400]

Bradley MM, Codispoti M, Cuthbert BN, Lang PJ, 2001. Emotion and motivation I: defensive and appetitive reactions in picture processing. Emotion. 1 (3), 276–298. 10.1037/1528-3542.1.3.276. [PubMed: 12934687]

Bradley MM, Lang PJ, 2000. Measuring emotion: behavior, feeling, and physiology. Cognitive Neuroscience of Emotion. Oxford University Press, pp. 242–276.

Bradley MM, Sabatinelli D, Lang PJ, Fitzsimmons JR, King W, Desai P, 2003. Activation of the visual cortex in motivated attention. Behav. Neurosci. 117 (2), 369–380. 10.1037/0735-7044.117.2.369. [PubMed: 12708533]

Buhle JT, Silvers JA, Wager TD, Lopez R, Onyemekwu C, Kober H, Weber J, Ochsner KN, 2014. Cognitive reappraisal of emotion: A meta-analysis of Human neuroimaging studies. Cerebral Cortex 24 (11), 2981–2990. 10.1093/cercor/bht154. [PubMed: 23765157]

Campbell BA, Wood G, McBride T, 1997. Origins of orienting and defensive responses: an evolutionary perspective. Attention and Orienting. Psychology Press.

Cavanagh JF, Frank MJ, 2014. Frontal theta as a mechanism for cognitive control. Trends Cogn. Sci. (Regul. Ed.) 18 (8), 414–421. 10.1016/j.tics.2014.04.012.

Codispoti M, de cesarei A, Ferrari V, 2023. Alpha-band oscillations and emotion: A review of studies on picture perception. Psychophysiology. 10.1111/psyp.14438.

Coombes SA, Janelle CM, Duley AR, 2005. Emotion and motor control: movement attributes following affective picture processing. J. Mot. Behav. 37 (6), 425–436. 10.3200/JMBR.37.6.425-436. [PubMed: 16280313]

Corbetta M, Shulman GL, 2002. Control of goal-directed and stimulus-driven attention in the brain. Nature Rev. Neurosci. 3 (3). 10.1038/nrn755. Article 3.

Cui Y, Versace F, Engelmann JM, Minnix JA, Robinson JD, Lam CY, Karam-Hage M, Brown VL, Wetter DW, Dani JA, Kosten TR, Cinciripini PM, 2013. Alpha oscillations in response to affective and cigarette-related stimuli in smokers. Nicotine Tobacco Res. 15 (5), 917–924. 10.1093/ntr/nts209.

Dalal SS, Sekihara K, Nagarajan SS, 2006. Modified beamformers for coherent source region suppression. IEEE Trans. Biomed. Eng. 53 (7), 1357–1363. 10.1109/TBME.2006.873752. [PubMed: 16830939]

De Cesarei A, Codispoti M, 2011. Affective modulation of the LPP and α-ERD during picture viewing. Psychophysiology. 48 (10), 1397–1404. 10.1111/j.1469-8986.2011.01204.x. [PubMed: 21486291]

Dell'Acqua C, Dal Bò E, Moretta T, Palomba D, Messerotti Benvenuti S, 2022. EEG time–frequency analysis reveals blunted tendency to approach and increased processing of unpleasant stimuli in dysphoria. Sci. Rep. 12 (1), 8161. 10.1038/s41598-022-12263-9. [PubMed: 35581359]

Diekhof EK, Kipshagen HE, Falkai P, Dechent P, Baudewig J, Gruber O, 2011. The power of imagination—How anticipatory mental imagery alters perceptual processing of fearful facial expressions. Neuroimage 54 (2), 1703–1714. 10.1016/j.neuroimage.2010.08.034. [PubMed: 20797441]

Dilks DD, Kamps FS, Persichetti AS, 2022. Three cortical scene systems and their development. Trends Cogn. Sci. (Regul. Ed.) 26 (2), 117–127. 10.1016/j.tics.2021.11.002.

Domes G, Schulze L, Böttger M, Grossmann A, Hauenstein K, Wirtz PH, Heinrichs M, Herpertz SC, 2010. The neural correlates of sex differences in emotional reactivity and emotion regulation. Hum. Brain Mapp. 31 (5), 758–769. 10.1002/hbm.20903. [PubMed: 19957268]

Du Y, Hua L, Tian S, Dai Z, Xia Y, Zhao S, Zou H, Wang X, Sun H, Zhou H, Huang Y, Yao Z, Lu Q, 2023. Altered beta band spatial-temporal interactions during negative emotional processing in major depressive disorder: an MEG study. J. Affect. Disord. 338, 254–261. 10.1016/j.jad.2023.06.001. [PubMed: 37271293]

Ernst MD, 2004. Permutation methods: A basis for exact inference. Statistical Sci. 19 (4), 676–685. 10.1214/088342304000000396.

Fanselow MS, 1994. Neural organization of the defensive behavior system responsible for fear. Psychon. Bull. Rev. 1 (4), 429–438. 10.3758/BF03210947. [PubMed: 24203551]

Fanselow MS, Dong H-W, 2010. Are the dorsal and ventral hippocampus functionally distinct structures? Neuron 65 (1), 7–19. 10.1016/j.neuron.2009.11.031. [PubMed: 20152109]

Ferrari V, Bradley MM, Codispoti M, Lang PJ, 2015. Massed and distributed repetition of natural scenes: brain potentials and oscillatory activity. Psychophysiology. 52 (7), 865–872. 10.1111/psyp.12424. [PubMed: 25847093]

Ferrari V, Canturi F, Codispoti M, 2022. Stimulus novelty and emotionality interact in the processing of visual distractors. Biol. Psychol. 167, 108238. 10.1016/j.biopsycho.2021.108238.

Foster BL, Koslov SR, Aponik-Gremillion L, Monko ME, Hayden BY, Heilbronner SR, 2022. A tripartite view of the posterior cingulate cortex. Nat. Rev. Neurosci. 24 (3), 173. 10.1038/s41583-022-00661-x. [PubMed: 36456807]

Friedl WM, Keil A, 2021. Aversive conditioning of spatial position sharpens neural population-level tuning in visual cortex and selectively alters alpha-band activity. J. Neurosci. 41 (26), 5723–5733. 10.1523/JNEUROSCI.2889-20.2021. [PubMed: 34035136]

Frijda NH, 2000. Emotions. International Handbook of Psychology. Sage Publications Ltd, pp. 207–222. 10.4135/9781848608399.n12.

Gaetz W, Liu C, Zhu H, Bloy L, Roberts TPL, 2013. Evidence for a motor gamma-band network governing response interference. Neuroimage 74. 10.1016/j.neuroimage.2013.02.013.

Gentili C, Cristea IA, Angstadt M, Klumpp H, Tozzi L, Phan KL, Pietrini P, 2016. Beyond emotions: A meta-analysis of neural response within face processing system in social anxiety. Exp. Biol. Med. 241 (3), 225–237. 10.1177/1535370215603514.

Grady CL, 2020. Meta-analytic and functional connectivity evidence from functional magnetic resonance imaging for an anterior to posterior gradient of function along the hippocampal axis. Hippocampus 30 (5), 456–471. 10.1002/hipo.23164. [PubMed: 31589003]

Grecucci A, Giorgetta C, Bonini N, Sanfey AG, 2013. Reappraising social emotions: the role of inferior frontal gyrus, temporo-parietal junction and insula in interpersonal emotion regulation. Front. Hum. Neurosci. 7. 10.3389/fnhum.2013.00523.

Grill-Spector K, Kourtzi Z, Kanwisher N, 2001. The lateral occipital complex and its role in object recognition. Vision. Res. 41 (10), 1409–1422. 10.1016/S0042-6989(01)00073-6. [PubMed: 11322983]

Gross J, Kujala J, Hämäläinen M, Timmermann L, Schnitzler A, Salmelin R, 2001. Dynamic imaging of coherent sources: studying neural interactions in the human brain. Proceed. National Acad. Sci. 98 (2), 694–699. 10.1073/pnas.98.2.694.

Gunduz A, Brunner P, Sharma M, Leuthardt EC, Ritaccio AL, Pesaran B, Schalk G, 2016. Differential roles of high gamma and local motor potentials for movement preparation and execution. Brain-Computer Interf. 3 (2), 88–102. 10.1080/2326263X.2016.1179087.

Güntekin B, Basar E, 2007. Emotional face expressions are differentiated with brain oscillations. Int. J. Psychophysiol. 64 (1), 91–100. 10.1016/j.ijpsycho.2006.07.003. [PubMed: 17156875]

Hanslmayr S, Staudigl T, Fellner M-C, 2012. Oscillatory power decreases and long-term memory: the information via desynchronization hypothesis. Front. Hum. Neurosci. 6. https://www.frontiersin.org/articles/10.3389/fnhum.2012.00074.

Heinrichs-Graham E, Wilson TW, 2015. Spatiotemporal oscillatory dynamics during the encoding and maintenance phases of a visual working memory task. Cortex 69, 121–130. 10.1016/j.cortex.2015.04.022. [PubMed: 26043156]

Herba CM, Landau S, Russell T, Ecker C, Phillips ML, 2006. The development of emotion-processing in children: effects of age, emotion, and intensity. J. Child Psychol. Psychiatry 47 (11), 1098–1106. 10.1111/j.1469-7610.2006.01652.x. [PubMed: 17076748]

Hillebrand A, Barnes GR, 2002. A quantitative assessment of the sensitivity of whole-head MEG to activity in the adult human cortex. Neuroimage 16, 638–650. 10.1006/nimg.2002.1102, 3 Pt 1. [PubMed: 12169249]

Hillebrand A, Singh KD, Holliday IE, Furlong PL, Barnes GR, 2005. A new approach to neuroimaging with magnetoencephalography. Hum. Brain Mapp. 25 (2), 199–211. 10.1002/hbm.20102. [PubMed: 15846771]

Hinojosa JA, Mercado F, Carretié L, 2015. N170 sensitivity to facial expression: A meta-analysis. Neurosci. Biobehav. Revi. 55, 498–509. 10.1016/j.neubiorev.2015.06.002.

Huster RJ, Stevens S, Gerlach AL, Rist F, 2009. A spectralanalytic approach to emotional responses evoked through picture presentation. Int. J. Psychophysiol. 72 (2), 212–216. 10.1016/j.ijpsycho.2008.12.009. [PubMed: 19135486]

Igelström KM, Graziano MSA, 2017. The inferior parietal lobule and temporoparietal junction: A network perspective. Neuropsychologia 105, 70–83. 10.1016/j.neuropsychologia.2017.01.001. [PubMed: 28057458]

Inuggi A, Sassi F, Castillo A, Campoy G, Leocani L, García Santos JM, Fuentes LJ, 2014. Cortical response of the ventral attention network to unattended angry facial expressions: an EEG source analysis study. Front. Psychol. 5. https://www.frontiersin.org/articles/10.3389/fpsyg.2014.01498.

Iordan MC, Greene MR, Beck DM, Fei-Fei L, 2015. Basic level category structure emerges gradually across Human ventral visual cortex. J. Cogn. Neurosci. 27 (7), 1427–1446. 10.1162/jocn_a_00790. [PubMed: 25811711]

Jabbi M, Keysers C, 2008. Inferior frontal gyrus activity triggers anterior insula response to emotional facial expressions. Emotion. 8 (6), 775–780. 10.1037/a0014194. [PubMed: 19102588]

Kastner S, Chen Q, Jeong SK, Mruczek REB, 2017. A brief comparative review of primate posterior parietal cortex: A novel hypothesis on the human toolmaker. Neuropsychologia 105, 123–134. 10.1016/j.neuropsychologia.2017.01.034. [PubMed: 28159617]

Keil A, Müller MM, Gruber T, Wienbruch C, Stolarova M, Elbert T, 2001. Effects of emotional arousal in the cerebral hemispheres: A study of oscillatory brain activity and event-related potentials. Clin. Neurophysiol.: Official J. Int. Federat. Clin. Neurophysiol. 112 (11), 2057–2068. 10.1016/s1388-2457(01)00654-x.

Keil A, Sabatinelli D, Ding M, Lang PJ, Ihssen N, Heim S, 2009. Re-entrant projections modulate visual cortex in affective perception: evidence from Granger causality analysis. Hum. Brain Mapp. 30 (2), 532–540. 10.1002/hbm.20521. [PubMed: 18095279]

Keil A, Stolarova M, Moratti S, Ray WJ, 2007. Adaptation in human visual cortex as a mechanism for rapid discrimination of aversive stimuli. Neuroimage 36 (2), 472. 10.1016/j.neuroimage.2007.02.048. [PubMed: 17451974]

Kiani R, Esteky H, Mirpour K, Tanaka K, 2007. Object category structure in response patterns of neuronal population in monkey inferior temporal cortex. J. Neurophysiol. 97 (6), 4296–4309. 10.1152/jn.00024.2007. [PubMed: 17428910]

Kim S-Y, Shin JE, Lee YI, Kim H, Jo HJ, Choi S-H, 2018. Neural evidence for persistent attentional bias to threats in patients with social anxiety disorder. Soc. Cogn. Affect. Neurosci. 13 (12), 1327–1336. 10.1093/scan/nsy101.

Kleiner M, Brainard D, Pelli D, Ingling A, Murray R, Broussard C, 2007. What's new in psychtoolbox-3. Perception. 36 (14), 1–16.

Klimesch W, 2012. Alpha-band oscillations, attention, and controlled access to stored information. Trends Cogn. Sci. (Regul. Ed.) 16 (12). 10.1016/j.tics.2012.10.007. Article 12.

Knyazev GG, Slobodskoj-Plusnin JY, Bocharov AV, 2009. Event-related delta and theta synchronization during explicit and implicit emotion processing. Neuroscience 164 (4), 1588–1600. 10.1016/j.neuroscience.2009.09.057. [PubMed: 19796666]

Knyazev GG, Slobodskoj-Plusnin JY, Bocharov AV, 2010. Gender differences in implicit and explicit processing of emotional facial expressions as revealed by event-related theta synchronization. Emotion. 10 (5), 678–687. 10.1037/a0019175. [PubMed: 21038950]

Kober H, Barrett LF, Joseph J, Bliss-Moreau E, Lindquist K, Wager TD, 2008. Functional grouping and cortical–subcortical interactions in emotion: A meta-analysis of neuroimaging studies. Neuroimage 42 (2), 998–1031. 10.1016/j.neuroimage.2008.03.059. [PubMed: 18579414]

Konorski J, 1967. Integrative Activity of the Brain: An Interdisciplinary Approach. University of Chicago Press.

Kovach CK, Gander PE, 2016. The demodulated band transform. J. Neurosci. Methods 261, 135–154. 10.1016/j.jneumeth.2015.12.004. [PubMed: 26711370]

Lang PJ, Bradley MM, 2010. Emotion and the motivational brain. Biol. Psychol. 84 (3), 437–450. 10.1016/j.biopsycho.2009.10.007. [PubMed: 19879918]

Lang PJ, Bradley MM, 2013. Appetitive and defensive motivation: goal-directed or goal-determined? Emotion Rev. 5 (3), 230–234. 10.1177/1754073913477511.

Lang PJ, Bradley MM, Cuthbert BN, 1990. Emotion, attention, and the startle reflex. Psychol. Rev. 97 (3), 377–395. 10.1037/0033-295X.97.3.377. [PubMed: 2200076]

Lang PJ, Bradley MM, Cuthbert BN, 1997a. International affective picture system (IAPS): technical manual and affective ratings. NIMH Center for the Study of Emotion and Attention 39–58.

Lang PJ, Bradley MM, Cuthbert BN, 1997b. Motivated attention: affect, activation, and action. Attention and Orienting. Psychology Press.

Lang PJ, McTeague LM, Bradley MM, 2016. RDoC, DSM, and the reflex physiology of fear: A bio-dimensional analysis of the anxiety disorders spectrum. Psychophysiology. 53 (3), 336–347. 10.1111/psyp.12462. [PubMed: 26877123]

Lee JY, Lindquist KA, Nam CS, 2017. Emotional granularity effects on event-related brain potentials during affective picture processing. Front. Hum. Neurosci. 11. 10.3389/fnhum.2017.00133.

Leech R, Sharp DJ, 2014. The role of the posterior cingulate cortex in cognition and disease. Brain 137 (1), 12–32. 10.1093/brain/awt162. [PubMed: 23869106]

Lew BJ, Fitzgerald EE, Ott LR, Penhale SH, Wilson TW, 2021. Three-year reliability of MEG resting-state oscillatory power. Neuroimage 243, 118516. 10.1016/j.neuroimage.2021.118516.

Li W, Keil A, 2023. Sensing fear: fast and precise threat evaluation in human sensory cortex. Trends Cogn. Sci. (Regul. Ed.) 27 (4), 341–352. 10.1016/j.tics.2023.01.001.

Lindquist KA, Wager TD, Kober H, Bliss-Moreau E, Barrett LF, 2012. The brain basis of emotion: A meta-analytic review. Behav. Brain Sci. 35 (3), 121–143. 10.1017/S0140525X11000446. [PubMed: 22617651]

Liu Y, Bengson J, Huang H, Mangun GR, Ding M, 2016. Top-down modulation of neural activity in anticipatory visual attention: control mechanisms revealed by simultaneous EEG-fMRI. Cerebral Cortex 26 (2), 517–529. 10.1093/cercor/bhu204. [PubMed: 25205663]

Luo Q, Holroyd T, Jones M, Hendler T, Blair J, 2007. Neural dynamics for facial threat processing as revealed by gamma band synchronization using MEG. Neuroimage 34 (2), 839–847. 10.1016/j.neuroimage.2006.09.023. [PubMed: 17095252]

Luo Q, Mitchell D, Cheng X, Mondillo K, Mccaffrey D, Holroyd T, Carver F, Coppola R, Blair J, 2009. Visual awareness, emotion, and gamma band synchronization. Cerebral Cortex 19 (8), 1896–1904. 10.1093/cercor/bhn216. [PubMed: 19047574]

Luther L, Horschig JM, van Peer JM, Roelofs K, Jensen O, Hagenaars MA, 2023. Oscillatory brain responses to emotional stimuli are effects related to events rather than states. Front. Hum. Neurosci. 16. 10.3389/fnhum.2022.868549.

MacNamara A, Klumpp H, Kennedy AE, Langenecker SA, Phan KL, 2017. Transdiagnostic neural correlates of affective face processing in anxiety and depression. Depress. Anxiety. 34 (7), 621–631. 10.1002/da.22631. [PubMed: 28453905]

Marchewka A, Żurawski Ł, Jednoróg K, Grabowska A, 2013. The Nencki Affective Picture System (NAPS): introduction to a novel, standardized, wide-range, high-quality, realistic picture database. Behav. Res. Methods 46 (2), 596. 10.3758/s13428-013-0379-1.

Maris E, Oostenveld R, 2007. Nonparametric statistical testing of EEG- and MEG-data. J. Neurosci. Methods 164 (1), 177–190. 10.1016/j.jneumeth.2007.03.024. [PubMed: 17517438]

Martini N, Menicucci D, Sebastiani L, Bedini R, Pingitore A, Vanello N, Milanesi M, Landini L, Gemignani A, 2012. The dynamics of EEG gamma responses to unpleasant visual stimuli: from local activity to functional connectivity. Neuroimage 60 (2), 922–932. 10.1016/j.neuroimage.2012.01.060. [PubMed: 22270349]

Marwick K, Hall J, 2008. Social cognition in schizophrenia: A review of face processing. Br. Med. Bull. 88 (1), 43–58. 10.1093/bmb/ldn035. [PubMed: 18812413]

McTeague LM, Lang PJ, 2012. The anxiety spectrum and the reflex physiology of defense: from circumscribed fear to broad distress. Depress. Anxiety. 29 (4), 264–281. 10.1002/da.21891. [PubMed: 22511362]

Meehan CE, Wiesman AI, Spooner RK, Schantell M, Eastman JA, Wilson TW, 2021. Differences in rhythmic neural activity supporting the temporal and spatial cueing of attention. Cerebral Cortex 31 (11), 4933–4944. 10.1093/cercor/bhab132. [PubMed: 34226925]

Meng X, Liu W, Zhang L, Li X, Yao B, Ding X, Yuan J, Yang J, 2016. EEG oscillation evidences of enhanced susceptibility to emotional stimuli during adolescence. Front. Psychol. 7. 10.3389/fpsyg.2016.00616.

Messerotti Benvenuti S, Buodo G, Mennella R, Dal Bò E, Palomba D, 2019.Appetitive and aversive motivation in depression: the temporal dynamics of task-elicited asymmetries in alpha oscillations. Sci. Rep. 9 (1), 17129. 10.1038/s41598-019-53639-8. [PubMed: 31748518]

Müller MM, Keil A, Gruber T, Elbert T, 1999. Processing of affective pictures modulates right-hemispheric gamma band EEG activity. Clin. Neurophysiol0 110 (11), 1913–1920. 10.1016/S1388-2457(99)00151-0.

Müller VI, Höhner Y, Eickhoff SB, 2018. Influence of task instructions and stimuli on the neural network of face processing: an ALE meta-analysis. Cortex 103, 240–255. 10.1016/j.cortex.2018.03.011. [PubMed: 29665467]

Murphy J, Devue C, Corballis PM, Grimshaw GM, 2020. Proactive control of emotional distraction: evidence from EEG alpha suppression. Front. Hum. Neurosci. 14. 10.3389/fnhum.2020.00318.

Noguchi Y, Kubo S, 2020. Changes in latency of brain rhythms in response to affective information of visual stimuli. Biol. Psychol. 149, 107787. 10.1016/j.biopsycho.2019.107787.

Ochsner KN, Gross JJ, 2005. The cognitive control of emotion. Trends Cogn. Sci. (Regul. Ed.) 9 (5), 242–249. 10.1016/j.tics.2005.03.010.

Öhman A, Lundqvist D, Esteves F, 2001. The face in the crowd revisited: A threat advantage with schematic stimuli. J. Pers. Soc. Psychol. 80 (3), 381–396. 10.1037/0022-3514.80.3.381. [PubMed: 11300573]

Öhman A, Wiens S, 2003. On the automaticity of autonomic responses in emotion: an evolutionary perspective. Handbook of Affective Sciences. Oxford University Press, pp. 256–275.

Ott LR, Penhale SH, Taylor BK, Lew BJ, Wang Y-P, Calhoun VD, Stephen JM, Wilson TW, 2021. Spontaneous cortical MEG activity undergoes unique age- and sex-related changes during the transition to adolescence. Neuroimage 244, 118552. 10.1016/j.neuroimage.2021.118552.

Panitz C, Keil A, Mueller EM, 2019. Extinction-resistant attention to long-term conditioned threat is indexed by selective visuocortical alpha suppression in humans. Sci. Rep. 9 (1), 15809. 10.1038/s41598-019-52315-1. [PubMed: 31676781]

Patel GH, Sestieri C, Corbetta M, 2019. The evolution of the temporoparietal junction and posterior superior temporal sulcus. Cortex 118, 38–50. 10.1016/j.cortex.2019.01.026. [PubMed: 30808550]

Pavlov YG, Kotchoubey B, 2022. Oscillatory brain activity and maintenance of verbal and visual working memory: A systematic review. Psychophysiology. 59 (5), e13735. 10.1111/psyp.13735.

Pei G, Xiao Q, Pan Y, Li T, Jin J, 2023. Neural evidence of face processing in social anxiety disorder: A systematic review with meta-analysis. Neurosci. Biobehav. Rev. 152, 105283. 10.1016/j.neubiorev.2023.105283.

Petro NM, Keil A, 2015. Pre-target oscillatory brain activity and the attentional blink. Exp. Brain Res. 233 (12), 3583–3595. 10.1007/s00221-015-4418-2. [PubMed: 26341931]

Petro NM, Livermore CL, Springer SD, Okelberry HJ, John JA, Glesinger R, Horne LK, Embury CM, Spooner RK, Taylor BK, Picci G, Wilson TW, 2025. Oscillatory brain dynamics underlying affective face processing. Soc. Cogn. Affect. Neurosci. 20 (1), nsaf047. 10.1093/scan/nsaf047.

Petro NM, Ott LR, Penhale SH, Rempe MP, Embury CM, Picci G, Wang Y-P, Stephen JM, Calhoun VD, Wilson TW, 2022. Eyes-closed versus eyes-open differences in spontaneous neural dynamics during development. Neuroimage 258, 119337. 10.1016/j.neuroimage.2022.119337.

Petro NM, Thigpen NN, Garcia S, Boylan MR, Keil A, 2019. Pre-target alpha power predicts the speed of cued target discrimination. Neuroimage 189, 878–885. 10.1016/j.neuroimage.2019.01.066. [PubMed: 30703522]

Petro NM, Tong TT, Henley DJ, Neta M, 2018. Individual differences in valence bias: fMRI evidence of the initial negativity hypothesis. Soc. Cogn. Affect. Neurosci. 13 (7), 687–698. 10.1093/scan/nsy049. [PubMed: 29931375]

Petro NM, Tottenham N, Neta M, 2021. Exploring valence bias as a metric for frontoamygdalar connectivity and depressive symptoms in childhood. Dev. Psychobiol. 1–16. 10.1002/dev.22084.

Pfurtscheller G, Klimesch W, 1992. Event-related synchronization and desynchronization of alpha and beta waves in a cognitive task. In: Başar E, Bullock TH (Eds.), Induced Rhythms in the Brain. Birkhäuser, pp. 117–128. 10.1007/978-1-4757-1281-0_6.

Picci G, Ott LR, Penhale SH, Taylor BK, Johnson HJ, Willett MP, Okelberry HJ, Wang Y, Calhoun VD, Stephen JM, Wilson TW, 2023. Developmental changes in endogenous testosterone have sexually-dimorphic effects on spontaneous cortical dynamics. Hum. Brain Mapp. 44 (17), 6043–6054. 10.1002/hbm.26496. [PubMed: 37811842]

Pitcher D, Garrido L, Walsh V, Duchaine BC, 2008. Transcranial magnetic stimulation disrupts the perception and embodiment of facial expressions. Journal of Neuroscience 28 (36), 8929–8933. 10.1523/JNEUROSCI.1450-08.2008. [PubMed: 18768686]

Poline J-B, Worsley KJ, Holmes AP, Frackowiak RSJ, Friston KJ, 1995. Estimating smoothness in statistical parametric maps: variability of p values. J. Comput. Assist. Tomogr. 19 (5), 788. [PubMed: 7560327]

Proskovec AL, Heinrichs-Graham E, Wiesman AI, McDermott TJ, Wilson TW, 2018. Oscillatory dynamics in the dorsal and ventral attention networks during the reorienting of attention. Hum. Brain Mapp. 39 (5), 2177–2190. 10.1002/hbm.23997. [PubMed: 29411471]

Proskovec AL, Heinrichs-Graham E, Wilson TW, 2016. Aging modulates the oscillatory dynamics underlying successful working memory encoding and maintenance. Hum. Brain Mapp. 37 (6), 2348–2361. 10.1002/hbm.23178. [PubMed: 26991358]

Proskovec AL, Heinrichs-Graham E, Wilson TW, 2019. Load modulates the alpha and beta oscillatory dynamics serving verbal working memory. Neuroimage 184, 256–265. 10.1016/j.neuroimage.2018.09.022. [PubMed: 30213775]

Ray WJ, Cole HW, 1985. EEG alpha activity reflects attentional demands, and beta activity reflects emotional and cognitive processes. Science (1979) 228 (4700), 750–752. [PubMed: 3992243]

Rempe MP, Casagrande CC, Embury CM, Arif Y, Bashford S, Garrison GM, Glesinger RJ, Okelberry HJ, Keifer EL, Picci G, Heinrichs-Graham E, Wilson TW, 2025. Hippocampal and cortical oscillatory dynamics reflect semantic processing and predict behavioral performance. J. Physiol. (Lond.).

Rennig J, Langenberger C, Karnath H-O, 2024. Beyond visual integration: sensitivity of the temporal-parietal junction for objects, places, and faces. Behav. Brain Functions 20 (1), 8. 10.1186/s12993-024-00233-2.

Roberts NA, Levenson RW, 2006. Subjective, behavioral, and physiological reactivity to ethnically matched and ethnically mismatched film clips. Emotion. 6 (4), 635–646. 10.1037/1528-3542.6.4.635. [PubMed: 17144754]

Sabatinelli D, Fortune EE, Li Q, Siddiqui A, Krafft C, Oliver WT, Beck S, Jeffries J, 2011. Emotional perception: meta-analyses of face and natural scene processing. Neuroimage 54 (3), 2524–2533. 10.1016/j.neuroimage.2010.10.011. [PubMed: 20951215]

Sabatinelli D, Frank DW, 2019. Assessing the primacy of Human amygdala-inferotemporal emotional scene discrimination with rapid whole-brain fMRI. Neuroscience 406, 212–224. 10.1016/j.neuroscience.2019.03.001. [PubMed: 30858109]

Sato W, Kochiyama T, Uono S, Matsuda K, Usui K, Inoue Y, Toichi M, 2011. Rapid amygdala gamma oscillations in response to fearful facial expressions. Neuropsychologia 49 (4), 612–617. 10.1016/j.neuropsychologia.2010.12.025. [PubMed: 21182851]

Schindler S, Bublatzky F, 2020. Attention and emotion: an integrative review of emotional face processing as a function of attention. Cortex 130, 362–386. 10.1016/j.cortex.2020.06.010. [PubMed: 32745728]

Schneirla TC, 1959. An evolutionary and developmental theory of biphasic processes underlying approach and withdrawal. Nebraska Symposium on Motivation, 1959. Univer. Nebraska Press, pp. 1–42.

Schubring D, Kraus M, Stolz C, Weiler N, Keim DA, Schupp H, 2020. Virtual reality potentiates emotion and task effects of alpha/beta brain oscillations. Brain Sci. 10 (8). 10.3390/brainsci10080537. Article 8.

Schubring D, Schupp HT, 2019. Affective picture processing: alpha- and lower beta-band desynchronization reflects emotional arousal. Psychophysiology. 56 (8), e13386. 10.1111/psyp.13386.

Schubring D, Schupp HT, 2021. Emotion and brain oscillations: high arousal is associated with decreases in alpha- and lower beta-band power. Cerebral Cortex 31 (3), 1597–1608. 10.1093/cercor/bhaa312. [PubMed: 33136146]

Schurz M, Radua J, Aichhorn M, Richlan F, Perner J, 2014. Fractionating theory of mind: A meta-analysis of functional brain imaging studies. Neurosci. Biobehav. Rev. 42, 9–34. 10.1016/j.neubiorev.2014.01.009. [PubMed: 24486722]

Simons RF, Detenber BH, Cuthbert BN, Schwartz DD, Reiss JE, 2003. Attention to television: alpha power and its relationship to image motion and emotional content. Media Psychol. 5 (3), 283–301. 10.1207/S1532785XMEP0503_03.

Singh KD, Barnes GR, Hillebrand A, Forde EME, Williams AL, 2002. Task-related changes in cortical synchronization are spatially coincident with the hemodynamic response. Neuroimage 16 (1), 103–114. 10.1006/nimg.2001.1050. [PubMed: 11969322]

Sollfrank T, Kohnen O, Hilfiker P, Kegel LC, Jokeit H, Brugger P, Loertscher ML, Rey A, Mersch D, Sternagel J, Weber M, Grunwald T, 2021. The effects of dynamic and static emotional facial expressions of humans and their avatars on the EEG: an ERP and ERD/ERS study. Front. Neurosci. 15. https://www.frontiersin.org/journals/neuroscience/articles/10.3389/fnins.2021.651044.

Springer SD, Okelberry HJ, Willett MP, Johnson HJ, Meehan CE, Schantell M, Embury CM, Rempe MP, Wilson TW, 2023. Age-related alterations in the oscillatory dynamics serving verbal working memory processing. Aging (Albany. NY) 15 (24), 14574–14590. 10.18632/aging.205403. [PubMed: 38154102]

Squire LR, Clark RE, Knowlton BJ, 2001. Retrograde amnesia. Hippocampus 11 (1), 50–55. 10.1002/1098-1063(2001)11:1<50. AID—HIPO1019>3.0. CO;2-G. [PubMed: 11261772]

Stevens JS, Hamann S, 2012. Sex differences in brain activation to emotional stimuli: A meta-analysis of neuroimaging studies. Neuropsychologia 50 (7), 1578–1593. 10.1016/j.neuropsychologia.2012.03.011. [PubMed: 22450197]

Taulu S, Simola J, 2006. Spatiotemporal signal space separation method for rejecting nearby interference in MEG measurements. Phys. Med. Biol. 51 (7), 1759–1768. 10.1088/0031-9155/51/7/008. [PubMed: 16552102]

Taylor SF, Liberzon I, Koeppe RA, 2000. The effect of graded aversive stimuli on limbic and visual activation. Neuropsychologia 38 (10), 1415–1425. 10.1016/s0028-3932(00)00032-4. [PubMed: 10869585]

Urry HL, 2006. Amygdala and ventromedial prefrontal cortex are inversely coupled during regulation of negative affect and predict the diurnal pattern of cortisol secretion among older adults. J. Neurosci. 26 (16), 4415–4425. 10.1523/JNEUROSCI.3215-05.2006. [PubMed: 16624961]

Uusitalo MA, Ilmoniemi RJ, 1997. Signal-space projection method for separating MEG or EEG into components. Med. Biol. Eng. Comput. 35 (2), 135–140. 10.1007/BF02534144. [PubMed: 9136207]

Uutela K, Taulu S, Hämäläinen M, 2001. Detecting and correcting for head movements in neuromagnetic measurements. Neuroimage 14 (6), 1424–1431. 10.1006/nimg.2001.0915. [PubMed: 11707098]

Van Veen BD, van Drongelen W, Yuchtman M, Suzuki A, 1997. Localization of brain electrical activity via linearly constrained minimum variance spatial filtering. IEEE Trans. Biomed. Eng. 44 (9), 867–880. 10.1109/10.623056. [PubMed: 9282479]

Vuilleumier P, 2005. How brains beware: neural mechanisms of emotional attention. Trends Cogn. Sci. (Regul. Ed.) 9 (12), 585–594. 10.1016/j.tics.2005.10.011.

Vuilleumier P, Pourtois G, 2007. Distributed and interactive brain mechanisms during emotion face perception: evidence from functional neuroimaging. Neuropsychologia 45 (1), 174–194. 10.1016/j.neuropsychologia.2006.06.003. [PubMed: 16854439]

Wager TD, Kang J, Johnson TD, Nichols TE, Satpute AB, Barrett LF, 2015. A bayesian model of category-specific emotional brain responses. PLoS. Comput. Biol. 11 (4), e1004066. 10.1371/journal.pcbi.1004066.

Wang X, Jin J, Liu W, Liu Z, Yin T, 2021. Emotional processing of sadness and disgust evoked by disaster scenes. Brain Behav. 11 (12), e2421. 10.1002/brb3.2421. [PubMed: 34807520]

Wiesman AI, Heinrichs-Graham E, Proskovec AL, McDermott TJ, Wilson TW, 2017. Oscillations during observations: dynamic oscillatory networks serving visuospatial attention. Hum. Brain Mapp. 38 (10), 5128–5140. 10.1002/hbm.23720. [PubMed: 28714584]

Wiesman AI, O'Neill J, Mills MS, Robertson KR, Fox HS, Swindells S, Wilson TW, 2018. Aberrant occipital dynamics differentiate HIV-infected patients with and without cognitive impairment. Brain 141 (6). 10.1093/brain/awy097. Article 6.

Wiesman AI, Wilson TW, 2019. The impact of age and sex on the oscillatory dynamics of visuospatial processing. Neuroimage 185, 513–520. 10.1016/j.neuroimage.2018.10.036. [PubMed: 30321644]

Worsley KJ, Marrett S, Neelin P, Vandal AC, Friston KJ, Evans AC, 1996. A unified statistical approach for determining significant signals in images of cerebral activation. Hum. Brain Mapp. 4 (1), 58–73. 10.1002/(SICI)1097-0193(1996)4:1<58. AID—HBM4>3.0.CO;2-O. [PubMed: 20408186]

Zaki J, Davis JI, Ochsner KN, 2012. Overlapping activity in anterior insula during interoception and emotional experience. Neuroimage 62 (1), 493–499. 10.1016/j.neuroimage.2012.05.012. [PubMed: 22587900]

Zhang D, Wang L, Luo Y, Luo Y, 2012. Individual differences in detecting rapidly presented fearful faces. PLoS. One 7 (11), e49517. 10.1371/journal.pone.0049517.

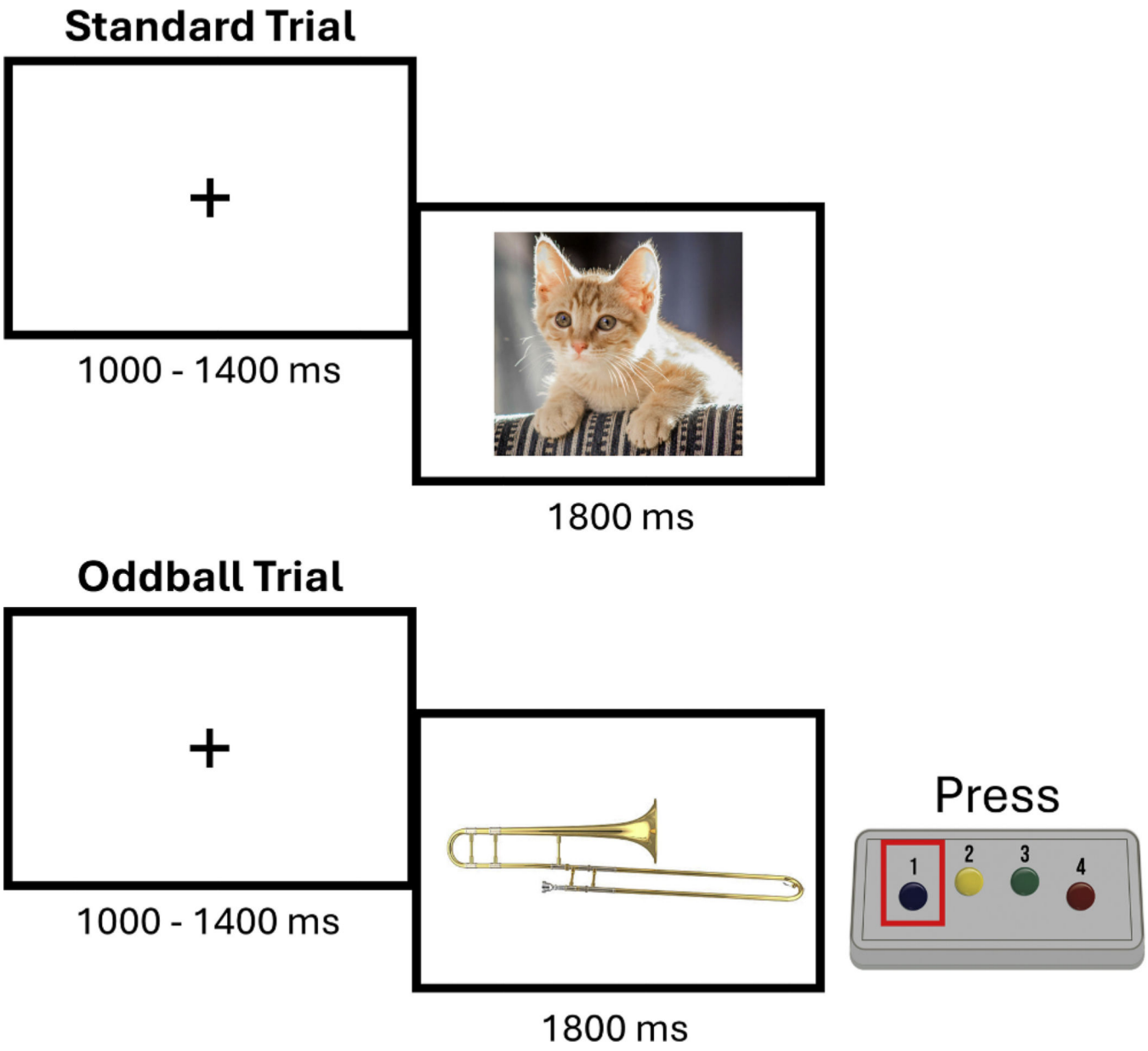

Fig. 1.

Emotional Image Processing Task. Following a fixation period that randomly varied from 1000 to 1400 ms and served as the baseline, emotional images were presented centrally for 1800 ms. The pictures on standard trials (top) were comprised of 100 unpleasant and 100 pleasant images of animals, landscapes, common objects and people, taken from the IAPS and NAPS stimuli sets. To gauge attention, 20 oddball trials containing a musical instrument (bottom) were presented and participants were asked to respond via button press. Oddball trials were excluded from analysis. Stimuli shown in this figure are for illustrative purposes only and not included in the task.

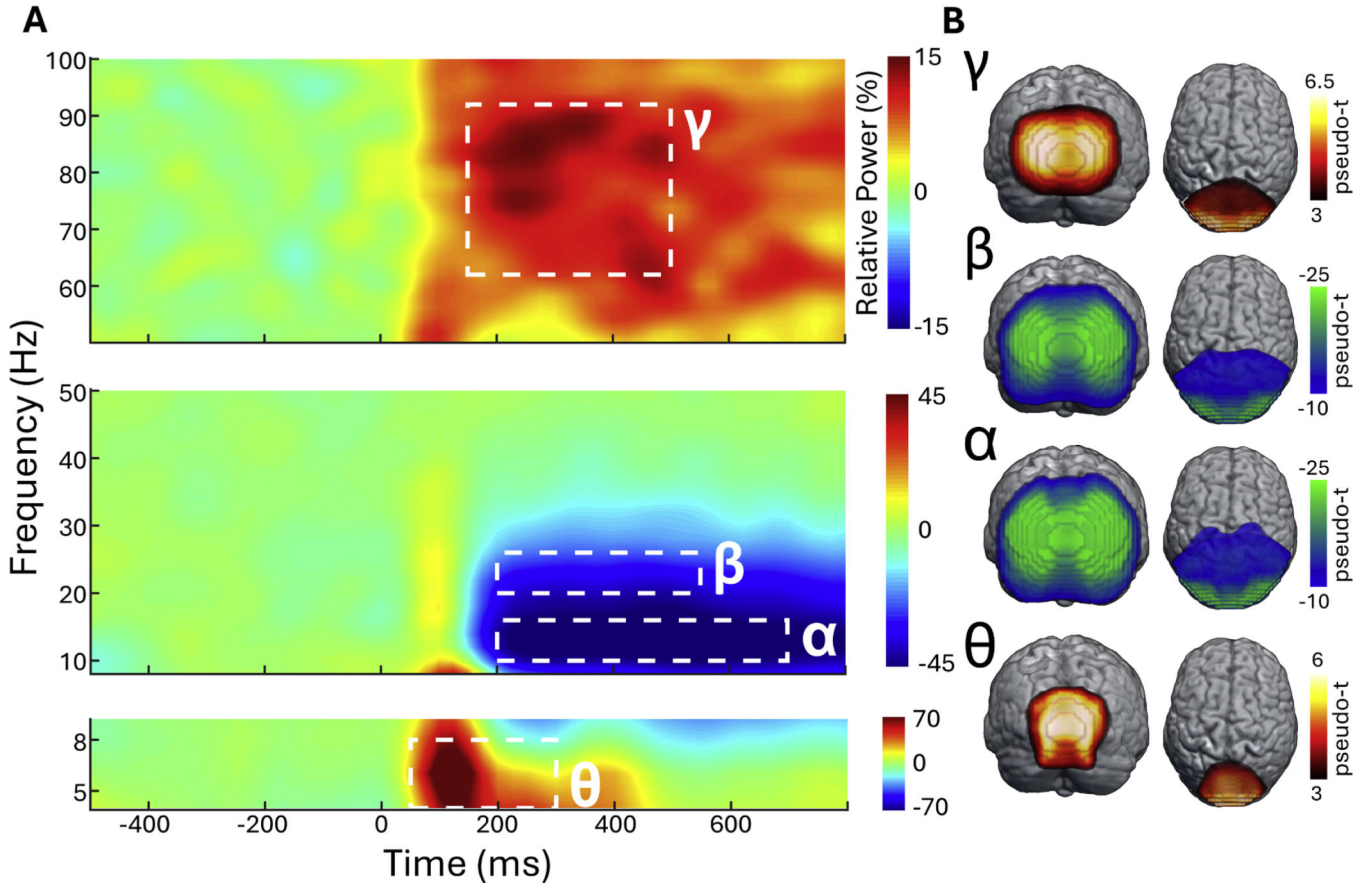

Fig. 2.

Sensor- and source-level oscillatory responses. (Left) Time-frequency spectrograms showing the grand-average oscillatory responses across all trials and participants from three representative MEG sensors. Time (ms) is shown on the x-axis and frequency (Hz) on the y-axis, with the color scale bar illustrating the change in oscillatory power relative to the baseline period. Strong increases in gamma (top; 1923) and theta (bottom; 2112) were observed, in addition to alpha and beta decreases (middle; 2512) from baseline. (Right) 3D renditions illustrating the grand-averaged images across all participants and both conditions (pseudo-t; see color bar) for each oscillatory response (i.e., time-frequency window).

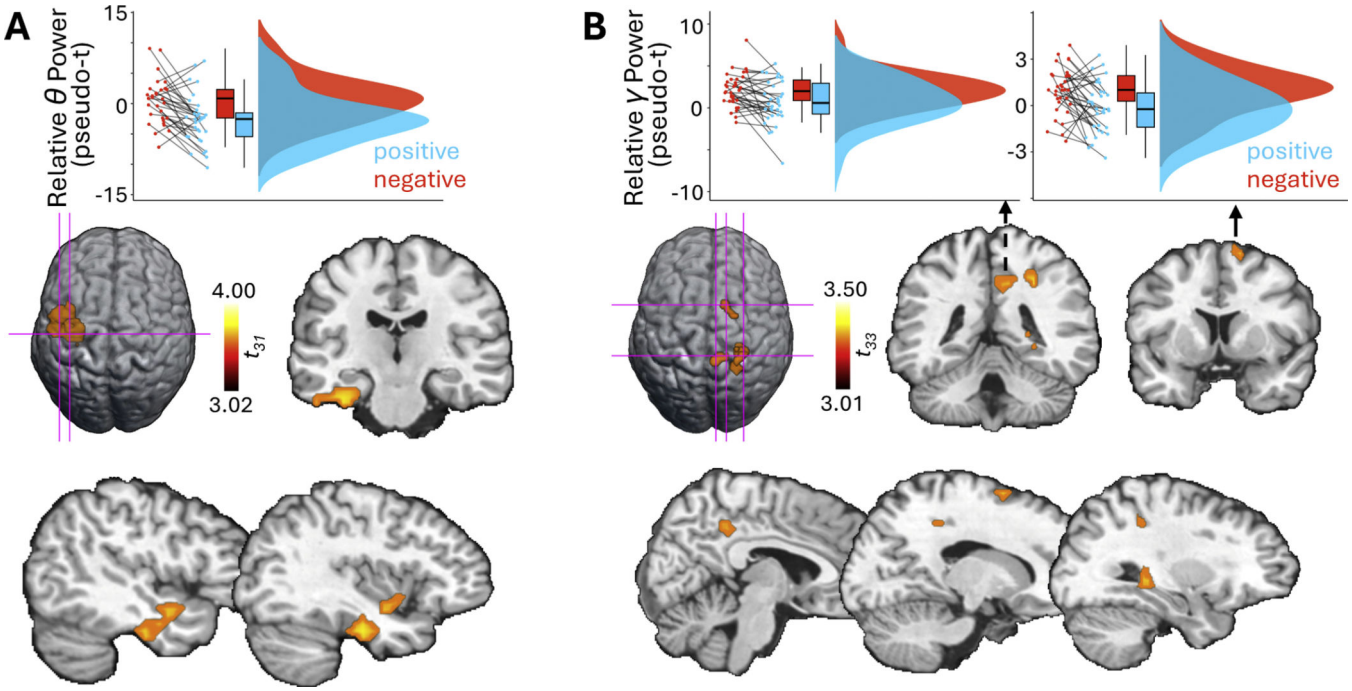

Fig. 3.

Differences in oscillatory activity between positive and negative images for the (A) theta and (B) gamma responses. In each panel, the brain images have been thresholded at $p < .005$, corrected, and illustrate cortical regions exhibiting significantly stronger responses during the negative compared to the positive images. In the data plots, dots represent the oscillatory power for each participant, with the negative condition shown in red connected to the positive condition shown in blue. The box plots show the mean, first and third quartiles, and the whiskers indicate the minima and maxima. Distribution plots illustrate the probability density.

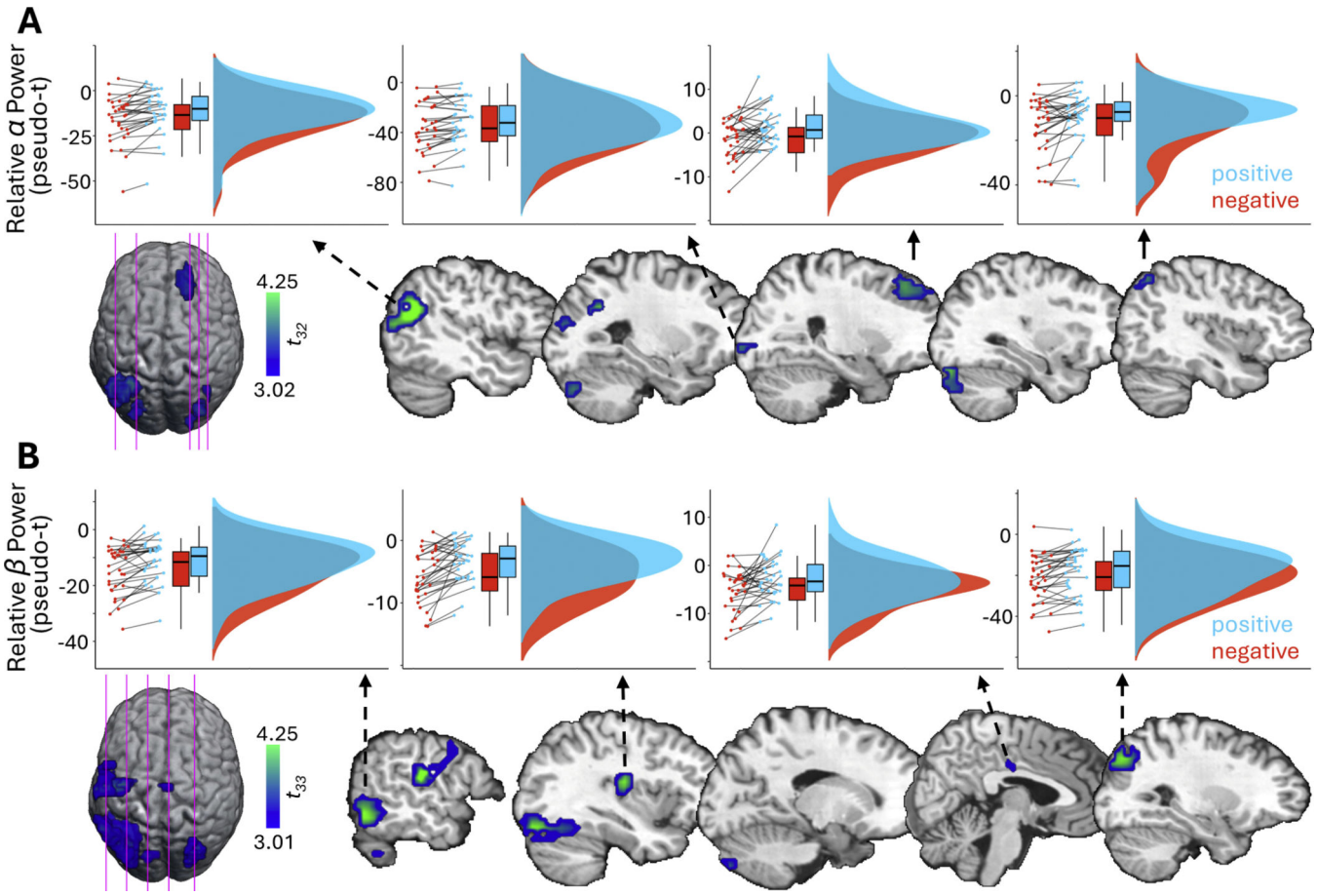

Fig. 4.

Differences in oscillatory activity between positive and negative images for the (A) alpha and (B) beta responses. In each panel, the brain images have been thresholded at $p < .005$, corrected, and illustrate cortical regions exhibiting significantly stronger oscillations (i.e., more negative relative to baseline) during the negative compared to the positive images. In the data plots, dots represent the oscillatory power per participant, with the negative condition shown in red connected to the positive condition shown in blue. The box plots show the mean, first and third quartiles, and the whiskers indicate the minima and maxima. Distribution plots illustrate the probability density.

Table 1

Significant negative > positive activations.

	Region	MNI			
		x	y	z	K
Theta					
	L Parahippocampal Gyrus	−40	−10	−25	111
Alpha					
	L Temporoparietal Junction	−38	−62	24	149
	R Inferior Occipital Gyrus	29	−86	−27	35
	R Superior Frontal Gyrus	18	20	49	63
	L Middle Occipital Gyrus	−30	−88	15	14
	R Superior Parietal Lobule	37	−68	49	10
	L Cerebellum	−27	−75	−40	16
	R Middle Occipital Gyrus	22	−99	−4	10
Beta					
	L Inferior Frontal Gyrus	−48	−20	16	127
	L Inferior Frontal Gyrus	−57	−59	−13	240
	R Inferior Parietal Cortex	25	−81	40	68
	L Cerebellum (posterior)	−15	−79	−49	16
	L Cerebellum (anterior)	−53	−45	−43	16
	R Middle Cingulate Gyrus	6	−17	35	10
Gamma					
	R Intraparietal Sulcus	22	−43	44	10
	R Hippocampus (posterior)	22	−33	20	38
	R Supplemental Motor Area	14	−1	68	12
	R Posterior Cingulate Cortex	10	−43	39	15